Optimal quantum strategy for locating Unruh channels

Qianqian Liu,[1] Tonghua Liu,[2,*] Cuihong Wen,[1,†] and Jieci Wang[1,‡]

[1]*Department of Physics and Synergetic Innovation Center for Quantum Effects, Key Laboratory of Low-Dimensional Quantum Structures and Quantum Control of Ministry of Education, and Key Laboratory for Matter Microstructure and Function of Hunan Province, Hunan Normal University, Changsha 410081, China*

[2]*School of Physics and Optoelectronic, Yangtze University, Jingzhou 434023, China*

(Received 11 January 2024; revised 2 July 2024; accepted 3 July 2024; published 19 August 2024)

From the perspective of quantum information theory, the effect of Unruh radiation on a two-level accelerated detector can be modeled as a quantum channel. In this work we employ the tools of channel-position finding to locate Unruh channels. The signal-idler and idler-free protocols are explored to determine the position of the target Unruh channel within a sequence of background channels. We derive the fidelity-based bounds for the ultimate error probability of each strategy and obtain the conditions where the signal-idler protocol is superior to the protocol involving idler-free states. It is found that the lower bound of the error probability for the signal-idler scheme exhibits clear advantages in all cases, while the idler-free scheme can only be implemented when the temperatures of the two channels are very close and the number of initial states is insufficient. Interestingly, it is shown that the optimal detection protocol relies on the residual correlations shared between the emitted probe state and the retained idler modes.

DOI: 10.1103/PhysRevA.110.022428

I. INTRODUCTION

The Unruh effect [1–4] is one of the most monumental achievements of quantum field theory in curved space-time. It plays a crucial role in the understanding of vacuum fluctuations and the nature of quantum thermal effects. It was predicted that a uniformly accelerated observer will detect a thermal bath by expressing the vacuum state in terms of a different set of operator bases defined along the timelike killing vector in their locally accelerated coordinate system [5–9]. A variety of techniques have been employed to analyze this phenomenon including the response of a two-level system, referred to as an Unruh-DeWitt (UD) detector [10–13], when it absorbs these thermal particles. Studying the Unruh effect from the perspective of quantum information theory not only could be helpful in understanding the Hawking effect [14–16], but also provides an explanation for the generation and degradation of entanglement in curved space-time [17–19]. The direct observation of the Unruh effect is considered as one of the key experimental goals of contemporary physics [20–24]. However, a simple calculation shows that an Unruh temperature of 1 K corresponds to an acceleration of the order of approximately 10^{21} m/s^2, which is extremely challenging to obtain [23,24]. In this sense, the technical obstacles to the detection of Unruh radiation lead to the indistinguishability of the Unruh channel in a general relativistic background.

On the other hand, quantum channels can model various physical processes [25,26], so the discrimination of different quantum channels [27–30] is a fundamental task in quantum information theory. The theory of channel-position finding (CPF) has been effectively used to determine the target channel with varying transmittance or induced noise within a range of background loss channels [28–30]. Recently, the advantages of quantum entanglement have been demonstrated in CPF, for example, the thermal loss channel [25] and the amplitude damping channel [31,32]. In this paper we study the task of determining the location of Unruh channels, in which different accelerations would induce differentiated responses in the detectors [10,11,13,33]. Using the UD detector model, the task of identifying the channel temperature difference is simplified to identifying the detector acceleration.

Here we focus on the problem of CPF under the constraint that the sources considered are comprised of at most one photon. Two protocols will be considered: the signal-idler (SI) protocol and idler-free (IF) protocol. In fact, in the applications of quantum sensing, the assistance of idler modes has been a crucial feature to achieve quantum enhanced performance [34,35], but the IF channel identification schemes have also received a great deal of attention because of their ability to eliminate quantum memory [29,36]. We consider two scenarios: (i) The temperature of the target channel is zero and it is located within a series of reference channels and (ii) the temperature difference between the target channel and the reference channel is particularly small. These two scenarios effectively encompass the potential background in which the target channel may exist. We establish fidelity-based bounds on the final error probability in the multiple-channel-discrimination problem and identify the quantum dominance involving various quantum sources. The main purpose of our study is to find the optimal strategy for locating the Unruh channels and the optimal operating conditions for different strategies.

*Contact author: liutongh@yangtzeu.edu.cn
†Contact author: cuihongwen@hunnu.edu.cn
‡Contact author: jcwang@hunnu.edu.cn

This paper is organized as follows. Section II outlines the Unruh channel-discrimination task. In Sec. III we calculate the detection error probability of the SI protocol and IF protocol for locating Unruh channels. Section IV compares the advantage of detection error probabilities between the SI protocol and the IF protocol. Section V presents a summary. Throughout the paper, we adopt the conventions $\hbar = G = c = \kappa_B = 1$.

II. UNRUH CHANNEL DISCRIMINATION TASK

A. Unruh channel

In this section we discuss the channel characterization of the Unruh effect on an accelerating detector. We consider a two-level semiclassical UD detector [10,11], where the detector follows a classical world line while its degrees of freedom remain quantum. For a two-qubit system involving Alice and Rob, the detectors carried by Alice remain static, while Rob's detector undergoes uniform acceleration a in the x direction and its duration of motion is denoted by Δ. The world line of Rob is described as

$$t(\tau) = a^{-1}\sinh a\tau, \quad x(\tau) = a^{-1}\cosh a\tau, \\ y(\tau) = z(\tau) = 0, \tag{1}$$

where τ is the acceleration detector proper time.

The initial state of the total system (detector plus field) is given by

$$\left|\Psi^{AR\phi}_{-\infty}\right\rangle = \left|\Psi^{AR}_{-\infty}\right\rangle \otimes |0_M\rangle, \tag{2}$$

where $|\Psi^{AR}_{-\infty}\rangle = \alpha|0_A\rangle|1_R\rangle + \beta|1_A\rangle|0_R\rangle$ defines the initial state shared by Alice's (A) and Rob's (R) detectors, with $|\alpha|^2 + |\beta|^2 = 1$. Here $|0_M\rangle$ represents that the external scalar field is in the Minkowski vacuum.

The total system Hamiltonian can be expressed as

$$H = H_A + H_R + H_{\rm KG} + H^{R\phi}_{\rm int}, \tag{3}$$

where $H_A = \Omega A^\dagger A$, $H_R = \Omega R^\dagger R$, Ω represents the detectors' energy gap, and $H_{\rm KG}$ represents the Hamiltonian for the free Klein-Gordon field. The accelerated detector Rob is coupled to a scalar field $\phi(x)$ through the interaction Hamiltonian [2]

$$H^{R\phi}_{\rm int}(t) = \epsilon(t)\int_{\Sigma_t} d^3\mathbf{x}\sqrt{-g}\phi(x)[\psi(\mathbf{x})R + \psi^*(\mathbf{x})R^\dagger], \tag{4}$$

where $g \equiv \det(g_{ab})$ and $\mathbf{x}$ represent the coordinates defined on the Cauchy surface $\Sigma_{t=\rm const}$ associated with some suitable timelike isometry. The smooth compact support real-valued function ϵ is introduced to ensure that the detector is active for a finite proper time interval Δ. For the purposes of this analysis, we consider the detector to be localized as given by the Gaussian $\psi(\mathbf{x}) = (\kappa\sqrt{2\pi})^{-3}\exp(-\mathbf{x}^2/2\kappa^2)$, where variance $\kappa = \text{const} \ll 1$ determines the width of the Gaussian state.

In the interaction picture, the final state $|\Psi^{AR\phi}_t\rangle$ describing the total system in the first-order perturbation is given by

$$\left|\Psi^{AR\phi}_t\right\rangle = [I + a^\dagger_{\rm RI}(\lambda)R - a_{\rm RI}(\bar\lambda)R^\dagger]\left|\Psi^{AR\phi}_{-\infty}\right\rangle, \tag{5}$$

where $|\Psi^{AR\phi}_{-\infty}\rangle$ is the corresponding initial state, $\lambda = -KEf$, $f \equiv \epsilon(t)\psi(\mathbf{x})e^{-i\Omega t}$, E is the difference between the advanced and retarded Green's functions, K is an operator that takes the positive-frequency part of the solutions of the Klein-Gordon equation with respect to the timelike isometry, and $a_{\rm RI}(\bar\lambda)$ and $a^\dagger_{\rm RI}(\lambda)$ represent the annihilation and creation operators for the λ mode, respectively. By inserting Eq. (2) into Eq. (5), we obtain

$$\left|\Psi^{AR\phi}_t\right\rangle = \left|\Psi^{AR\phi}_{-\infty}\right\rangle + \alpha|0_A\rangle|0_R\rangle \otimes [a^\dagger_{\rm RI}(\lambda)|0_M\rangle] + \beta|1_A\rangle|1_R\rangle \\ \otimes [a_{\rm RI}(\bar\lambda)|0_M\rangle]. \tag{6}$$

The Bogoliubov transformations between the Rindler operators and the operators annihilating the Minkowski vacuum can be expressed as [10,11]

$$a_{\rm RI}(\bar\lambda) = \frac{a_M(\overline{F_{1\Omega}}) + e^{-\pi\Omega/a}a^\dagger_M(F_{2\Omega})}{(1-e^{-2\pi\Omega/a})^{1/2}}, \\ a^\dagger_{\rm RI}(\lambda) = \frac{a^\dagger_M(F_{1\Omega}) + e^{-\pi\Omega/a}a_M(\overline{F_{2\Omega}})}{(1-e^{-2\pi\Omega/a})^{1/2}}, \tag{7}$$

where $F_{1\Omega} = \frac{\lambda + e^{-\pi\Omega/a}\lambda\circ w}{(1-e^{-2\pi\Omega/a})^{1/2}}$, $F_{2\Omega} = \frac{\overline{\lambda\circ w} + e^{-\pi\Omega/a}\bar\lambda}{(1-e^{-2\pi\Omega/a})^{1/2}}$, and $w(t,x) = (-t,-x)$ represents the wedge reflection isometry.

The reduced density matrix of the two-qubit state is obtained by tracing out the degrees of freedom associated with the scalar field

$$\rho^{AR}_t = \left\|\Psi^{AR\phi}_t\right\|^{-2}\mathrm{Tr}_\phi\left|\Psi^{AR\phi}_t\right\rangle\left\langle\Psi^{AR\phi}_t\right| \\ = \begin{pmatrix} \mathcal{C} & 0 & 0 & 0 \\ 0 & |\alpha|^2\mathcal{A} & \alpha\beta\mathcal{A} & 0 \\ 0 & \alpha\beta\mathcal{A} & |\beta|^2\mathcal{A} & 0 \\ 0 & 0 & 0 & \mathcal{B} \end{pmatrix}, \tag{8}$$

where

$$\mathcal{A} = \frac{1-q}{(1-q)+\nu^2(|\alpha|^2+|\beta|^2q)}, \\ \mathcal{B} = \frac{\nu^2|\beta|^2q}{(1-q)+\nu^2(|\alpha|^2+|\beta|^2q)}, \\ \mathcal{C} = \frac{\nu^2|\alpha|^2}{(1-q)+\nu^2(|\alpha|^2+|\beta|^2q)}, \tag{9}$$

with the parametrized acceleration $q \equiv e^{-2\pi\Omega/a}$. The effective coupling between the detector and the scalar field is $\nu^2 \equiv \|\lambda\|^2 = \frac{\epsilon^2\Omega\Delta}{2\pi}e^{-\Omega^2\kappa^2}$ [8,10,11,13], where $\Omega^{-1} \ll \Delta$ is necessary for the validity of the above definition. In the present work the coupling parameter is constrained to $\nu^2 \ll 1$ to ensure the validity of the perturbative approach. Notably, q is a monotonic function of the acceleration a, and $q \to 0$ corresponds to zero acceleration and zero temperature. These facts suggest that the Unruh effect can be interpreted as a noisy quantum channel.

The dynamics of open quantum systems can be characterized as follows. The evolution from the initial state $\rho^{AR}_{-\infty}$ to the final state ρ^{AR}_t can alternatively be expressed as

$$\rho^{AR}_t = U(t)\rho^{AR}_{-\infty}U^\dagger(t), \tag{10}$$

where $U(t)$ is the propagator of the joint system dynamics from the initial time to the final time. The object of interest is the subsystem R, whose state at any times t is governed by the standard quantum-mechanical prescription through the

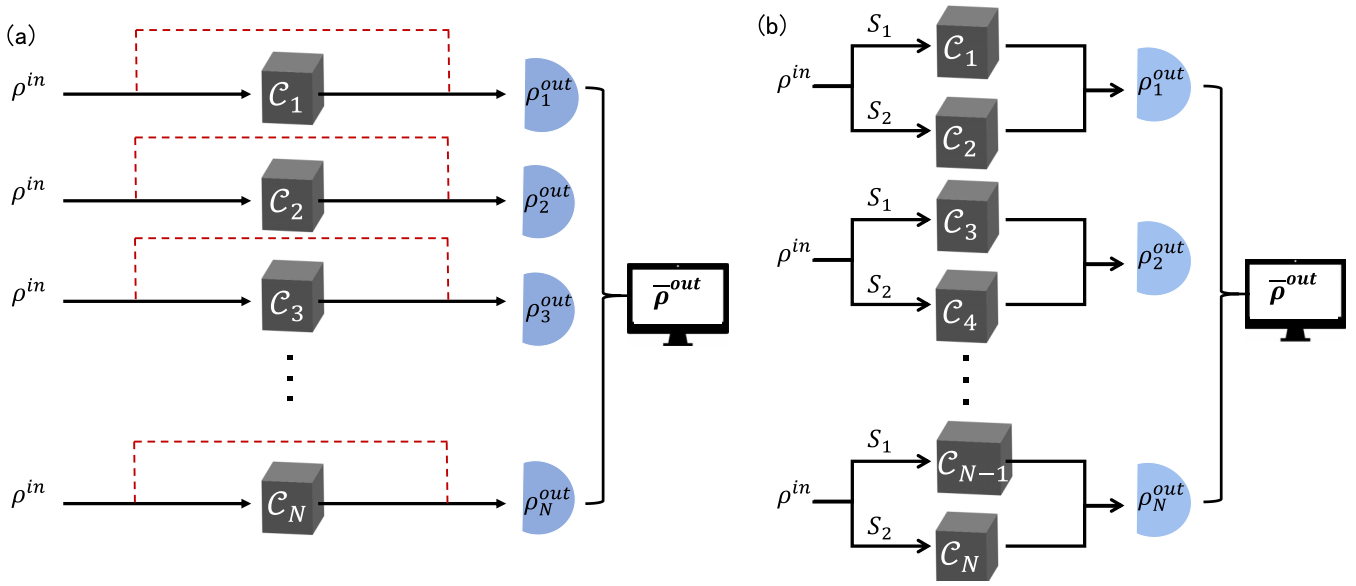

FIG. 1. Our setup for the CPF protocol that provides a benchmark for the general quantum channel. We assume N boxes, consisting of a target channel and $N-1$ reference channels. Two different protocols for the CPF of the Unruh channel are employed: (a) the signal-idler protocol of the CPF and (b) the idler-free protocol of the CPF for biphoton states.

following quantum dynamical process:

$$\rho_t^R = \mathrm{Tr}_B\big[U(t)\rho_{-\infty}^{AR}U^\dagger(t)\big]. \tag{11}$$

The quantum dynamical process can be represented by the quantum map $\mathcal{C}_\rho$ defined as

$$\mathcal{C}_\rho = \sum_j^\infty M_j^R \rho_0 M_j^{R\dagger}, \tag{12}$$

where ρ_0 is an initial state and M_j^R represents an operator for different dynamical evolution processes. Based on the preceding analysis and calculations, the Unruh channel with operators M_j^R acting on Rob can be characterized by the Choi matrix

$$M_1^R = \begin{pmatrix} \sqrt{1-q} & 0 \\ 0 & \sqrt{1-q} \end{pmatrix}, \quad M_2^R = \begin{pmatrix} 0 & 0 \\ \nu\sqrt{q} & 0 \end{pmatrix},$$
$$M_3^R = \begin{pmatrix} 0 & \nu \\ 0 & 0 \end{pmatrix}. \tag{13}$$

Accelerated quantum systems interacting with fields inevitably undergo the quantum dynamics of the Unruh effect. This quantum process can be characterized by the parametrized acceleration q and the effective coupling parameter ν. We consider the subsystem ρ_t^A, where M^A represents an identical operator because the detector of Alice remains static and switched off. The operator form derivation of the channel is independent of the form of the initial state.

B. Quantum channel discrimination

In this section we employ the tools of CPF involving $N \geqslant 2$ boxes to locate the target Unruh channel position. As shown in Fig. 1, the boxes $\mathcal{C}_i$ $(i = 1, 2, \ldots, N)$ are modeled as Unruh channels with different temperatures. The target channel $\mathcal{C}_\mathcal{T}$ occupies one box with the parametrized acceleration q_i, while the other $N-1$ boxes represent the reference channel $\mathcal{C}_\mathcal{R}$ with the parametrized acceleration $q_{j\neq i}$. Identification of the target Unruh channel is a symmetric hypothesis testing problem where the task is to discriminate between N hypotheses given by [37,38]

$$H_i : \mathcal{C}_i = \mathcal{C}_\mathcal{T}, \quad \mathcal{C}_{j\neq i} = \mathcal{C}_\mathcal{R}. \tag{14}$$

At the transmitter, the initial state ρ^{in} is injected into each of the boxes. Each channel is represented by an accelerated detector which interacts with its surroundings [13], and this detection process can be described as a quantum map for the quantum state. The task of correctly identifying the target channel in a series of reference channels may be reduced to distinguishing the possible channel outputs [28–30]. The ability to do this accurately, with a low error probability, directly relates to an ability to determine the correct result. Channel patterns are probed using $M \gg 1$ identical and independent copies of some input probe state $\rho^{\mathrm{in}\otimes M}$. After M pattern interactions, an optimized positive-operator-valued measure is employed for the classification. The detection error probability $p_{\mathrm{err}}^{N,M}(\rho)$ refers to the error probability of incorrectly identifying the target channel from a series of reference channels, constituting a discriminant problem involving N boxes and M identical transmissions of different types. Exact analytical forms of the error probability are challenging to compute except for a few specific quantum states [38,39]. However, the upper and lower bounds of the error probability are easier to calculate, which are

$$p_{\mathrm{err}}^{N,M}(\rho) \leqslant p_{\mathrm{err}}^{\mathrm{U}} = \sum_{n'>n} \sqrt{p_{n'}p_n}[F(\rho,\sigma)]^{2M} \tag{15}$$

and

$$p_{\mathrm{err}}^{N,M}(\rho) \geqslant p_{\mathrm{err}}^{\mathrm{L}} = \tfrac{1}{2}\sum_{n'>n} p_{n'}p_n[F(\rho,\sigma)]^{4M}, \tag{16}$$

where $F(\rho,\sigma)$ is the Bures fidelity [40,41]

$$F(\rho,\sigma) := \|\sqrt{\rho}\sqrt{\sigma}\|_1 = \mathrm{tr}\sqrt{\sqrt{\rho}\sigma\sqrt{\rho}}. \tag{17}$$

It is assumed that all slices may occur with equal probability, so we get $p_n = \frac{1}{N}$ for any N. Then we get the simplified boundary

$$p_{\mathrm{err}}^{\mathrm{U}} = (N-1)[F(\mathcal{C}_{\mathcal{T}},\mathcal{C}_{\mathcal{R}})]^{2M}, \tag{18}$$

$$p_{\mathrm{err}}^{\mathrm{L}} = \frac{N-1}{2N}[F(\mathcal{C}_{\mathcal{T}},\mathcal{C}_{\mathcal{R}})]^{4M}. \tag{19}$$

III. DETECTION ERROR PROBABILITIES

A. Signal-idler protocol

We first employ the SI strategy to locate the target Unruh channels. This protocol has been proved effective in discriminating Gaussian lossy channels [25,26,30–32]. As depicted in Fig. 1(a), an entanglement-based quantum source is given by a tensor product over all the boxes ($\bigotimes N$), where each signal S_i (black) box is entangled with an ancillary idler I_i (red). The input state for each box is a maximally entangled state

$$|\Psi^{\mathrm{in}}\rangle = \frac{1}{\sqrt{2}}(|00\rangle + |11\rangle). \tag{20}$$

Only the signal probes the box, while the idler state is directly sent to the receiver for combination with the output. The associated quantum channel is expressed as

$$\mathcal{E}_i^N := \bigotimes_{j\neq i}(\mathcal{C}_{\mathcal{R}\,j}\otimes\mathcal{I}_{I_j})\otimes(\mathcal{C}_{\mathcal{T}\,i}\otimes\mathcal{I}_{I_i}). \tag{21}$$

Upon the action of an Unruh channel only on the signal mode while performing the identity on the reference idler mode, we obtain the density operator of the output state

$$\rho^{\mathrm{out}} = \frac{1-q}{2}(|00\rangle\langle 00| + |00\rangle\langle 11| + |11\rangle\langle 00| + |11\rangle\langle 11|) + \frac{\nu^2}{2}|01\rangle\langle 01| + \frac{q\nu^2}{2}|10\rangle\langle 10|. \tag{22}$$

Computing the fidelity between two output states under differing Unruh channels with the parametrized acceleration q_1 and q_2, which correspond to accelerations a_1 and a_2, respectively, we obtain

$$F\left(\rho_{q_1}^{\mathrm{out}},\rho_{q_2}^{\mathrm{out}}\right) = \tfrac{1}{4}[4(-1+q_1)(-1+q_2)+(1+q_1q_2)\nu^4] + \tfrac{1}{4}\Big[\sqrt{-4(-2+q_1)q_1-\left(1+q_1^2\right)\nu^4} \times\sqrt{-4(-2+q_2)q_2-\left(1+q_2^2\right)\nu^4}\Big]. \tag{23}$$

By inserting Eq. (23) into Eqs. (18) and (19), the error probability for the SI protocol is then lower and upper bounded by

$$p_{\mathrm{err}}^{N,M}(\rho) \geqslant p_{\mathrm{err}}^{\mathrm{SI,L}} = \frac{N-1}{2N}\left[F\left(\rho_{q_1}^{\mathrm{out}},\rho_{q_2}^{\mathrm{out}}\right)\right]^{4M} \tag{24}$$

and

$$p_{\mathrm{err}}^{N,M}(\rho) \leqslant p_{\mathrm{err}}^{\mathrm{SI,U}} = (N-1)\left[F\left(\rho_{q_1}^{\mathrm{out}},\rho_{q_2}^{\mathrm{out}}\right)\right]^{2M}, \tag{25}$$

respectively.

B. Idler-free protocol

Now we consider the IF protocol without idler mode reservation. In this case, the two-mode state ρ^{in} serves as probes into two adjacent boxes, with the modes labeled as signals S_1 and S_2, as illustrated in Fig. 1(b). While the optimal quantum strategy for various scenarios, such as quantum illumination [35,42,43], spectroscopy [44], and quantum readings [45], often involves an entangled idler-assisted protocol, the storage of the idler mode poses a challenging task. The character of IF protocols lies in their ease of implementation and the absence of considerations for memory construction. Therefore, investigating the IF strategy is valuable, as it will help us understand whether quantum superiority can still be achieved even without a quantum memory for storing the idler mode.

In the IF protocol setup, we take advantage of the complete entanglement exhibited with the Bell state in the multichannel array to achieve quantum advantage. For any CPF problem consisting of $N \geqslant 4$ (even) individual channels, the global quantum channel acting on the initial state is

$$\mathcal{E}_i^{N/2} := \bigotimes_{j\neq i}(\mathcal{C}_{\mathcal{R}\,j}\otimes\mathcal{C}_{\mathcal{R}\,j})\otimes(\mathcal{C}_{\mathcal{T}\,i}\otimes\mathcal{C}_{\mathcal{R}i}). \tag{26}$$

If both modes S_1 and S_2 pass through two Unruh channels with the same parametrized acceleration q_1, the final state at the output is

$$\rho_{q_1,q_1}^{\mathrm{out}} = \tfrac{1}{2}\begin{pmatrix} Q_1^2+\nu^4 & 0 & 0 & Q_1^2 \\ 0 & Q_1\nu^2+Q_1q_1\nu^2 & 0 & 0 \\ 0 & 0 & Q_1\nu^2+Q_1q_1\nu^2 & 0 \\ Q_1^2 & 0 & 0 & Q_1^2+q_1^2\nu^4 \end{pmatrix}, \tag{27}$$

where $Q_1 = 1-q_1$. If the two modes of the initial state ρ^{in} pass through two Unruh channels with the parametrized accelerations q_1 and q_2, the final state at the output takes the form

$$\rho_{q_2,q_1}^{\mathrm{out}} = \tfrac{1}{2}\begin{pmatrix} Q_1Q_2+\nu^4 & 0 & 0 & Q_1Q_2 \\ 0 & Q_1\nu^2+Q_2q_1\nu^2 & 0 & 0 \\ 0 & 0 & Q_2\nu^2+Q_1q_2\nu^2 & 0 \\ Q_1Q_2 & 0 & 0 & Q_1Q_2+q_1q_2\nu^4 \end{pmatrix}, \tag{28}$$

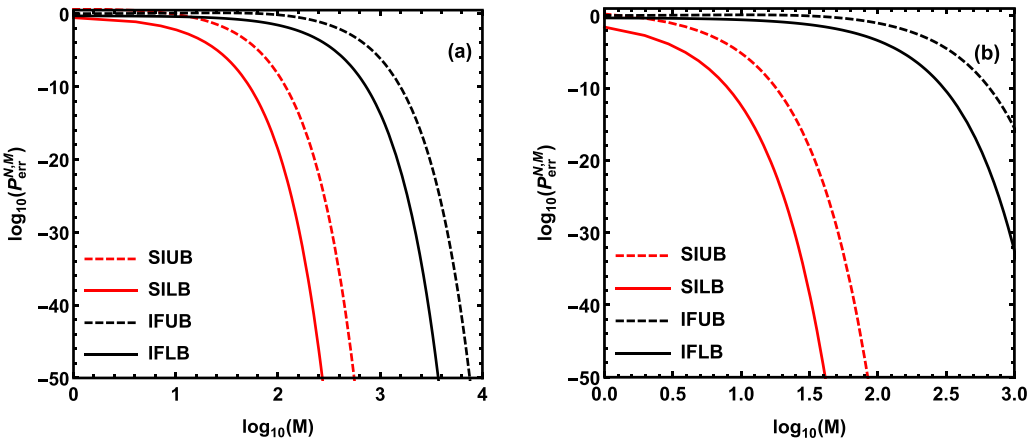

FIG. 2. Quantum channel-position-finding error probability $P_{\rm err}^{N,M}$ with $N = 4$ versus the number of uses M for two types of protocols: a Bell biphoton state in both a signal-idler (red) and an idler-free (black) setup. The detection error probability of the target channel with zero acceleration is among reference channels with (a) $q_1 = 0.1$ and (b) $q_1 = 0.5$.

where $Q_2 = 1 - q_2$. The lower and upper bounds for the error probabilities of the correct channel pair, calculated based on the fidelity between the two output states mentioned, are [30]

$$\tilde{p}_{\rm err}^{N,M}(\rho) \geqslant \tilde{p}_{\rm err}^{\rm IF,L} = \frac{N-2}{2N}\left[F\left(\rho_{q_1,q_1}^{\rm out}, \rho_{q_2,q_1}^{\rm out}\right)\right]^{4M} \tag{29}$$

and

$$\tilde{p}_{\rm err}^{N,M}(\rho) \leqslant \tilde{p}_{\rm err}^{\rm IF,U} = \frac{N-2}{2}\left[F\left(\rho_{q_1,q_1}^{\rm out}, \rho_{q_2,q_1}^{\rm out}\right)\right]^{2M}. \tag{30}$$

The objective of the CPF task is to determine the location of the target channel, rather than merely identifying the pair containing it. In an IF protocol, the first stage involves successfully identifying the correct pair and the second stage entails engineering a secondary CPF protocol by combining the correct pair with two additional reference channels. This enables us to pinpoint the location of the target channel. To maintain the energy constraint, we choose to divide the total number of probes into two parts, generating $M/2$ probes for each stage of the IF strategy in the CPF process.

Considering this two-stage approach, there are two ways in which an overall error can occur. The first scenario involves misidentifying the pair where the target channel is located in the initial stage, resulting in a failure to accomplish the task of locating the target channel. The second scenario involves correctly identifying the pair in which the target channel is located in the first stage, but in the second stage, there is an incorrect identification of which of the two channels is the target channel. Therefore, we can utilize the relevant lower and upper bounds to derive the final error probability of the IF scheme as follows:

$$\begin{aligned} &p_{\rm err}^{N,M/2}(|\psi_2\rangle\langle\psi_2|) \\ &\quad = \tilde{p}_{\rm err}^{N,M/2}(|\psi_2\rangle\langle\psi_2|) + \left[1 - \tilde{p}_{\rm err}^{N,M/2}(|\psi_2\rangle\langle\psi_2|)\right]\tilde{p}_{\rm err}^{4,M/2} \\ &\qquad \times (|\psi_2\rangle\langle\psi_2|). \end{aligned} \tag{31}$$

The $p_{\rm err}^{\rm IF,U}$ and $p_{\rm err}^{\rm IF,L}$ are obtained by combining Eqs. (29)–(31).

IV. QUANTUM ADVANTAGE OF THE SIGNAL-IDLER STRATEGY

In the preceding section we utilized the two-energy level detector as a thermometer model and the theory of CPF for discriminating the Unruh temperature. As mentioned earlier, to find the most effective method for detecting the Unruh channel, we need to compare the upper and lower bounds of error probabilities associated with different protocols. Denoting the upper and lower bounds of the SI (IF) protocols by $p_{\rm err}^{\rm SI,U}$ and $p_{\rm err}^{\rm SI,L}$ ($p_{\rm err}^{\rm IF,U}$ and $p_{\rm err}^{\rm IF,L}$), respectively, we define the minimum guaranteed advantage (MGA) as the minimum performance enhancement achieved by a SI strategy over the IF one [41],

$$\Delta p_{\rm err}^{\rm min} := p_{\rm err}^{\rm IF,L} - p_{\rm err}^{\rm SI,U}. \tag{32}$$

If $\Delta p_{\rm err}^{\rm min} > 0$, the advantage of the SI strategy is guaranteed. One can also define the maximum potential advantage (MPA) as follows:

$$\Delta p_{\rm err}^{\rm max} := p_{\rm err}^{\rm IF,L} - p_{\rm err}^{\rm SI,L}. \tag{33}$$

This represents the maximum potential improvement that quantum strategies can provide when the derived lower bound is fundamental.

If the target channel is a zero-acceleration channel within a series of Unruh reference channels, the probe scheme performance is illustrated in Fig. 2. It can be seen that for a given M, the error probabilities of $p_{\rm err}^{\rm SI,U}$ and $p_{\rm err}^{\rm SI,L}$ are both lower than $p_{\rm err}^{\rm IF,L}$. This result shows that the error probabilities bound in the SI protocol offer robust advantages, including both the MGA and MPA, along with a scaling advantage in the error exponent. Figures 2(a) and 2(b) show that this conclusion remains valid regardless of whether the reference channel is cryogenic or high temperature. We also find that the MGA function, which guarantees the advantage of the SI, increases as the number of copies of transmitted modes M increases.

If the single target channel is subjected to a nonzero parametrized acceleration $q_2 = q_1 + 0.01$, the temperatures of the target channel and the reference channel become very close, which makes it difficult to distinguish. Figure 3 illustrates the detection error probabilities versus the number

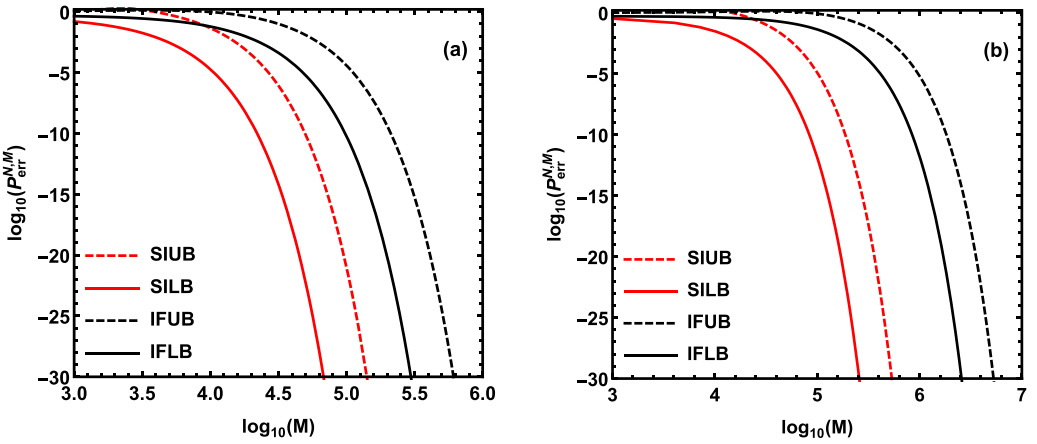

FIG. 3. Quantum channel-position-finding error probability $P_{\rm err}^{N,M}$ with $N = 4$ versus the number of uses M for two types of protocols: a Bell biphoton state in both a signal-idler (red) and an idler-free (black) setup. The detection error probability of the target channel with nonzero parametrized acceleration ($q_2 = q_1 + 0.01$) is among reference channels with (a) $q_1 = 0.1$ and (b) $q_1 = 0.5$.

of modes M for the SI and IF protocols. When resolving two Unruh temperature channels, the SI scheme requires a larger number of copies M compared to the IF scheme, which exhibits both the MPA and MGA. We can conclude that the IF protocols for channel localization are only feasible with a small number of copy probes, in which $p_{\rm err}^{\rm SI,U}$ is greater than $p_{\rm err}^{\rm IF,L}$. This demonstrates that a lower probability of detection error can be achieved by increasing the number of copy states. Comparing Figs. 3(a) and 3(b), we observe that both schemes perform well in locating a range of cryogenic reference channels, given that high temperatures tend to attenuate the initial quantum correlation.

Based on the analysis, we observe that the SI scheme exhibits significant advantages in the CPF task of Unruh channels, particularly when employing a large number of copy states. Upon performing the calculations, it becomes evident that the residual quantum correlation of the final state in the SI scheme surpasses that of the IF scheme, enhancing its efficiency in distinguishing between different channels. In other words, the similarity between the signal and idler states reduces the error probability of the CPF task. However, it is worth noting that the IF protocol eliminates the need for idler assistance to achieve quantum advantages in some of the most relevant discrimination scenarios, thereby relaxing practical requirements for prominent quantum sensing applications.

V. CONCLUSION

This paper has presented performance comparisons among various channel position schemes for the CPF problem, considering channels with different temperatures. Our detection scheme is conducted under energy constraints, specifically utilizing an average of only one photon per channel for detection of the entire channel array. We consider the geometric characterization of the Unruh channel, where each channel is represented as an operator resulting from the interaction of an UD with its environment. We investigate the task of determining the location of two or more given quantum channels by exploring the SI and IF protocols. The objective is to pinpoint the position of a target Unruh channel within a sequence of reference channels.

In the task of locating between two Unruh channels, we calculated the output fidelity of CPF to test multiple quantum hypotheses. This provides upper and lower bounds on the error probability, even in cases of small differences in channel temperature and the number of probe states is insufficient. When performing the task of distinguishing the zero-temperature channel and the Unruh channel, we stressed that the SI strategy outperforms the IF strategy, exhibiting both MGA and MPA across entire value regions. When resolving the target channel and reference channel with very close temperatures, the IF scheme is effective only in a scenario with a very low number of copy probes. These findings not only demonstrate that augmenting the number of copy probes can exponentially enhance the efficiency of the detection strategy, but also offer a theoretical framework for laboratories to employ diverse detection protocols for detection tasks. We hope that our results will stimulate further research on the discrimination of quantum operations. Our main lesson is that the residual feeble quantum correlation may offer an enormous performance advantage despite its being used in an entanglement-breaking scenario.

ACKNOWLEDGMENTS

This work was supported by the National Natural Science Foundation of China under Grants No. 12122504, No. 12203009, No. 12374408, and No. 12035005; the Natural Science Foundation of Hunan Province under Grant No. 2023JJ30384; and the Hunan provincial major sci-tech program under Grant No. 2023ZJ1010.

[1] W. G. Unruh, Phys. Rev. D **14**, 870 (1976).
[2] W. G. Unruh and R. M. Wald, Phys. Rev. D **29**, 1047 (1984).
[3] L. C. B. Crispino, A. Higuchi, and G. E. A. Matsas, Rev. Mod. Phys. **80**, 787 (2008).

[4] W. G. Brenna, E. G. Brown, R. B. Mann, and E. Martín-Martínez, Phys. Rev. D **88**, 064031 (2013).
[5] I. Fuentes-Schuller and R. B. Mann, Phys. Rev. Lett. **95**, 120404 (2005).
[6] E. Martín-Martínez, I. Fuentes, and R. B. Mann, Phys. Rev. Lett. **107**, 131301 (2011).
[7] E. Martín-Martínez and J. León, Phys. Rev. A **80**, 042318 (2009).
[8] R. M. Wald, *Quantum Field Theory in Curved Spacetimes and Black Hole Thermodynamics* (University of Chicago Press, Chicago, 1994).
[9] J. Wang and J. Jing, Phys. Rev. A **82**, 032324 (2010).
[10] A. G. S. Landulfo and G. E. A. Matsas, Phys. Rev. A **80**, 032315 (2009).
[11] L. C. Céleri, A. G. S. Landulfo, R. M. Serra, and G. E. A. Matsas, Phys. Rev. A **81**, 062130 (2010).
[12] X. Liu, Z. Tian, J. Wang, and J. Jing, Phys. Rev. D **97**, 105030 (2018).
[13] J. Wang, Z. Tian, J. Jing, and H. Fan, Phys. Rev. A **93**, 062105 (2016).
[14] S. W. Hawking, Nature (London) **248**, 30 (1974).
[15] G. W. Gibbons and S. W. Hawking, Phys. Rev. D **15**, 2738 (1977).
[16] M. Kalinski, Laser Phys. **15**, 1367 (2005).
[17] Q. Liu, S.-M. Wu, C. Wen, and J. Wang, Sci. China Phys. Mech. Astron. **66**, 120413 (2023).
[18] S.-M. Wu, H.-S. Zeng, and T. Liu, New J. Phys. **24**, 073004 (2022).
[19] A. Mukherjee, S. Gangopadhyay, and A. S. Majumdar, Phys. Rev. D **108**, 085018 (2023).
[20] W. G. Unruh, Phys. Rep. **307**, 163 (1998).
[21] R. Schützhold, G. Schaller, and D. Habs, Phys. Rev. Lett. **97**, 121302 (2006).
[22] Z. Tian, J. Wang, J. Jing, and A. Dragan, Ann. Phys. (NY) **377**, 1 (2017).
[23] E. T. Akhmedov and K. Gubarev, arXiv:2310.02866.
[24] I. Peña and D. Sudarsky, Found. Phys. **44**, 689 (2014).
[25] J. L. Pereira, Q. Zhuang, and S. Pirandola, Phys. Rev. Res. **2**, 043189 (2020).
[26] Q. Zhuang and S. Pirandola, Phys. Rev. Lett. **125**, 080505 (2020).
[27] M. F. Sacchi, Phys. Rev. A **72**, 014305 (2005).
[28] Q. Zhuang and S. Pirandola, Commun. Phys. **3**, 103 (2020).
[29] J. L. Pereira, L. Banchi, Q. Zhuang, and S. Pirandola, Phys. Rev. A **103**, 042614 (2021).
[30] A. Karsa, J. Carolan, and S. Pirandola, Phys. Rev. A **105**, 023705 (2022).
[31] A. Arqand, L. Memarzadeh, and S. Mancini, Phys. Rev. A **102**, 042413 (2020).
[32] M. Rexiti and S. Mancini, J. Phys. A: Math. Theor. **54**, 165303 (2021).
[33] D. Ahn, Phys. Rev. A **98**, 022308 (2018).
[34] S. Lloyd, Science **321**, 1463 (2008).
[35] S. H. Tan, B. I. Erkmen, V. Giovannetti, S. Guha, S. Lloyd, L. Maccone, S. Pirandola, and J. H. Shapiro, Phys. Rev. Lett. **101**, 253601 (2008).
[36] C. Harney and S. Pirandola, npj Quantum Inf. **7**, 153 (2021).
[37] E. Bagan, J. A. Bergou, S. S. Cottrell, and M. Hillery, Phys. Rev. Lett. **116**, 160406 (2016).
[38] D. Qiu and L. Li, Phys. Rev. A **81**, 042329 (2010).
[39] S. Zhang, Y. Feng, X. Sun, and M. Ying, Phys. Rev. A **64**, 062103 (2001).
[40] R. Jozsa, J. Mod. Opt. **41**, 2315 (1994).
[41] C. Harney, L. Banchi, and S. Pirandola, Phys. Rev. A **103**, 052406 (2021).
[42] A. Karsa, G. Spedalieri, Q. Zhuang, and S. Pirandola, Phys. Rev. Res. **2**, 023414 (2020).
[43] R. Nair and M. Gu, Optica **7**, 771 (2020).
[44] H. Shi, Z. Zhang, S. Pirandola, and Q. Zhuang, Phys. Rev. Lett. **125**, 180502 (2020).
[45] S. Pirandola, Phys. Rev. Lett. **106**, 090504 (2011).